Sn-Doped Hematite Nanoparticles for Potential Photocatalytic Dye Degradation

Svetlana Em[1], Mussa Yedigenov[1], Laura Khamkhash[2], Anara Molkenova[1], Timur Sh. Atabaev[1]

[1]Department of Chemistry, Nazarbayev University, Astana 010000, Kazakhstan
[2]Nazarbayev University Core Facilities, Astana 010000, Kazakhstan

timur.atabaev@nu.edu.kz

Abstract. Recently, low-cost hematite (α-Fe_2O_3) metal oxide semiconductor has attracted enormous attention for the photoelectrochemical water splitting and photocatalytic applications. The main purpose of this work is to study the effects of Sn-doping on the photocatalytic properties of hematite nanoparticles (NPs). Morphology and physicochemical properties of prepared samples were analyzed using X-ray diffraction analysis (XRD), transmission electron microscope (TEM), and UV-vis spectroscopy. Rhodamine B (RB) dye was used as a model organic pollutant to test the photocatalytic activity of prepared samples. It was found that the photocatalytic activity of Sn-doped hematite NPs was higher than that of the undoped hematite NPs. The recyclability tests suggested that 3 mol% Sn-doped hematite NPs can be used as a promising reusable photocatalyst for dyes degradation.

1. Introduction

Recently, pollution of water resources with organic dyes has grown significantly due to textile and dye manufacturing industries. The photocatalytic decomposition of organic pollutants on the surface of semiconductor nanostructures can be considered as one of the effective methods of wastewater treatment. In particular, electron-hole pairs can be generated in semiconductor nanostructure under the sunlight illumination followed by generation of the highly reactive OH radicals. These highly reactive OH radicals degrade the organic pollutants and attack the microorganisms, bacteria, fungi, etc. [1]. Thus, wastewater purification from organic pollutants and disinfection can be performed simultaneously. To date, various metal oxide micro-/nanostructures such as TiO_2 [2], ZnO [3], $SrTiO_3$ [4], WO_3 [5], and SnO_2 [6] have been widely used as photocatalysts for dye degradation. On the other hand, TiO_2, ZnO, $SrTiO_3$, WO_3, and SnO_2 have relatively large bandgaps, thus, mainly absorb only UV and part of the blue spectrum. Therefore, extending the absorption range of photocatalyst towards the visible spectrum will be highly beneficial in terms of construction of a low-cost photocatalytic reactor. In this reactor, the photocatalyst can utilize the solar photons only to purify and disinfect the wastewater. In this regard, the hematite (α-Fe_2O_3) can be a promising material because of its excellent chemical stability, low-cost, abundance and suitable bandgap range (1.9-2.2 eV). On the other hand, high recombination rate and poor conductivity are seriously limiting the widespread applications of hematite as a photocatalyst [7]. To resolve these issues, hematite can be doped with some elements such as Ti [7], Sn [8], Ni and Zn [9], Mo and Cr [10], etc. Previous study suggested that Sn-doping (5%) can significantly improve the conductivity and charge transfer in hematite film [8]. On the other hand, hematite for photocatalytic degradation of pollutants must be sufficiently small in size to achieve high surface area and shorten the pathway of the photogenerated charge carriers to the surface.

To the best of our knowledge, the synthesis of Sn-doped hematite nanoparticles by combustion method has been not reported so far. Thus, the synthesis of Sn-doped hematite using a facile combustion method was reported in this study. Furthermore, the effects of Sn-doping concentration on the photocatalytic properties of hematite were investigated in this study.

2. Materials and Methods

$Fe(NO_3)_3 \cdot 9H_2O$ (INN, ≥98%), Polyethylene glycol (PEG, Mn = 400), and $SnCl_2 \cdot 2H_2O$ (TCD, ≥98%) were purchased from Sigma-Aldrich and used as received. In a typical preparation procedure, 9.68 g of INN and 1 g of PEG were dissolved in 50 ml of deionized water. Next, various amounts of TCD (0, 1, 3, and 5 mol% of Sn in relation to Fe) were added to the solution under vigorous stirring. The prepared solution was dried at 80 ^{o}C for 24 h, and then inserted into a preheated furnace (550 ^{o}C) for 1 h. The obtained foamy mass was collected, crushed in the agate mortar and then used as a photocatalyst.

Rhodamine B (RB) dye was used as a model pollutant dye to evaluate the photocatalytic activity of prepared Sn-doped hematite NPs. In particular, 1 g of the photocatalyst was added to the 100 ml of RB solution (20 mg/L) in a glass vessel. First, the mixture was stirred for 30 min in the dark to reach the equilibrium adsorption-desorption state between the RB and photocatalyst surface. Next, H_2O_2 (1 ml, 30%) as an oxidant was also added to the mixture solution under continuous stirring. The solution was then exposed to the simulated light from a xenon lamp (300 W). Every 15 min, 2 ml of the solution was removed from the mixture solution for analysis. The RB dye degradation rate was monitored at the 553 nm using the UV-vis. All measurements were performed at room temperature.

3. Results and discussion

The morphology and size distribution of prepared samples were analyzed using a TEM. Figure 1 shows the typical images of (a) undoped and (b) 3 mol% Sn-doped hematite NPs. The majority of formed NPs have a scabrous quasi-spherical form with size distribution from ~ 30 to 180 nm, however, particles with bigger sizes were also observed. One can see that Sn-doped hematite NPs in average have slightly smaller size than undoped hematite NPs. The average size reduction was probably due to Sn-doping effects and observed also for other Sn-doped hematite NPs (not shown here).
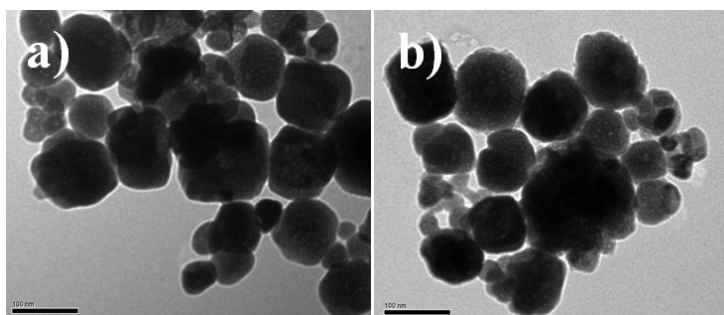

Figure 1. TEM images of (a) undoped and (b) 3 mol% Sn-doped hematite NPs.

XRD analysis was performed to confirm the formation of hematite structure. Figure 2 shows the typical XRD patterns of hematite NPs doped with different Sn concentrations. All detected peaks were easily indexed to the rhombohedral phase of α-Fe_2O_3 (JCPDS No. 33-0664) [7]. One can see that the prepared samples were highly crystalline since sharp and narrow peaks were observed. In addition, no impurity peaks were detected, suggesting that Sn was probably doped into a hematite matrix due to low concentration.
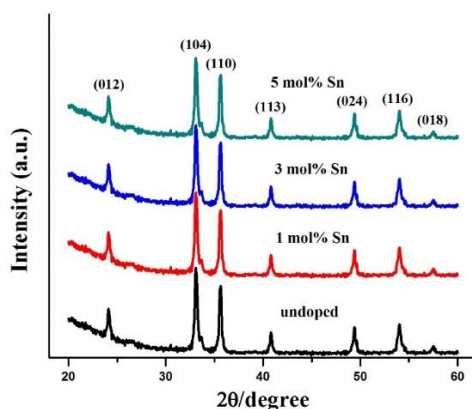
Figure 2. XRD patterns of hematite NPs doped with different Sn concentrations.

The mean crystallite sizes for all samples were calculated by Scherrer's equation. It was found that the mean crystallite sizes decrease as the Sn-concentration increasing (33.7; 31.2; 29.4; and 27.1 nm for 0, 1, 3 and 5 mol% doped samples). The size reduction can be associated with Sn atoms that can locate near/in hematite boundaries and decrease the diffusion rate. As a consequence, the mean crystallite size of the Sn-doped samples become smaller than that of the undoped one. EDX elemental mapping was employed to confirm the successful Sn-doping. Figure 3 shows the mapping results of 1 mol% Sn-doped hematite NPs taken over a relatively large area. One can see that all three elements, i.e. Fe, O, and Sn were detected, even though the sample with small doping concentration was tested (1 mol% Sn). According to the distribution uniformity, it can be concluded that Sn element was uniformly doped into a hematite NPs.
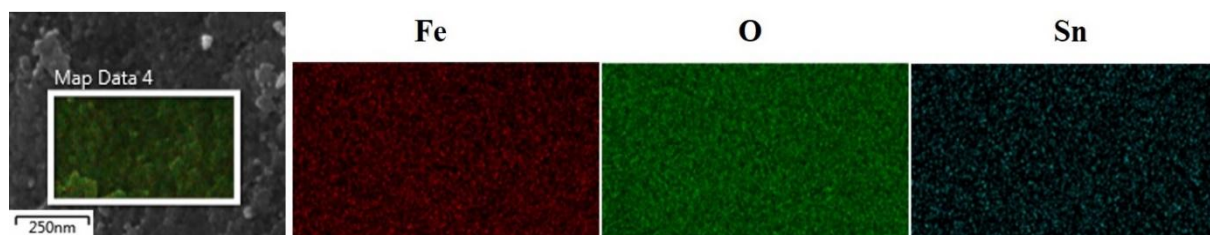

Figure 3. EDX elemental mapping of 1 mol% Sn-doped hematite NPs.

To investigate the photocatalytic activity of prepared Sn-doped hematite NPs, RB dye was used as a model pollutant for degradation. Figure 4 shows the degradation of RB without and with the presence of Sn-doped hematite NPs under constant simulated light illumination for 1 hour. It was found that without the photocatalyst addition RB concentration was decreased to about 89%. On the other hand, enhanced degradation rate was observed when photocatalyst was added to the solution. For example, the concentration of RB decreased to about 61 % in the presence of undoped hematite NPs. In case of the doped hematite NPs, the degradation rate was found to be Sn-concentration dependent. In hematite nanostructure, increased donor concentration can be formed at low Sn concentration when Fe^{3+} substituted with Sn^{4+}. The increased donor concentration suppresses the electron-hole recombination rate and improves the hematite conductivity [7-10]. On the other hand, high Sn concentration may decrease the conductivity and increase the recombination rate due to numerous defects in the hematite structure. In addition, Sn-doped hematite has enhanced absorption in visible region because of the reduced bandgap [8]. Therefore, the observed improved photocatalytic activity can be attributed to the numerous of factors such as: a) high surface area, b) improved conductivity, c) reduction of electron-hole charge recombination, d) bandgap alteration. It is obvious that 3 mol% Sn-doped hematite NPs have higher photocatalytic activity compared to other samples (RB concentration decreased to around 33%). Thus, 3 mol% Sn-doped hematite NPs was considered as an optimal doping concentration for Sn-doped hematite NPs prepared by this method. Hematite NPs with optimal

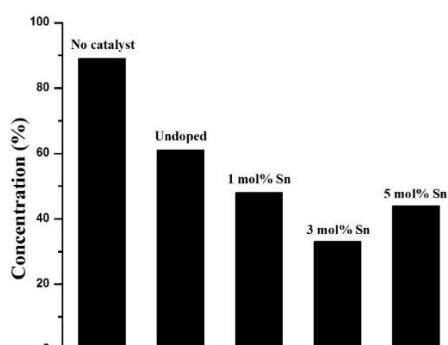doping concentration was further used for time-dependent degradation rate and recyclability experiments.

Figure 4. Degradation of RB dye without and with the photocatalyst under constant simulated light illumination for 1 hour.

The time-dependent degradation rate of colorant can be expressed using the following equation:

$$I = C/C_0 \times 100\%$$

where, I – signal intensity (a.u.), C_0 – initial concentration of RB dye, and C – concentration at any time moment. It is obvious that the peak intensity depends on the amount of RB dye in solution. Thus, with gradual degradation of RB dye the absorption intensity decrease too. The absorbance intensity of RB was monitored at maximum point (553 nm). Figure 5 shows the normalized time-dependent degradation rate of RB dye in dark conditions, without and with 3 mol% Sn-doped hematite NPs. It was found that no changes occur with RB dye in dark conditions. The RB was partially self-degraded (89% remain after 1 h of constant light illumination). On the other hand, the degradation rate increased significantly with addition of photocatalyst (33% remain after 1 h of constant light illumination). Thus, we concluded that dye pollutants degraded more efficiently in the presence of Sn-doped hematite NPs.
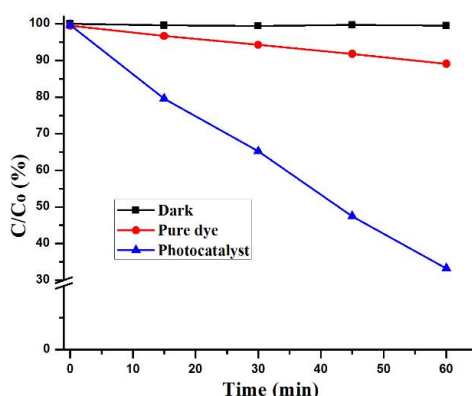

Figure 5. Time-dependant photocatalytic degradation of RB under constant light illumination.

The photocatalytic activity of the recycled sample (3 mol% Sn-doped hematite NPs) was tested under the same conditions more than three times. No significant changes (deviation $\leq$ 6%) were observed, indicating that prepared sample can be reusable.

4. Conclusions
In summary, a combustion method was used to fabricate Sn-doped hematite NPs. It was shown that the photocatalytic properties of hematite NPs are strongly depended on the Sn concentration. According to the experimental study, 3 mol% Sn-doped hematite has the highest photocatalytic

activity compared to other samples. In addition, the reusability tests showed that 3 mol% Sn-doped hematite NPs can be successfully used several times under the direct solar light illumination.

Acknowledgements

References

[1]   Linsebigler A L, Lu G, Yates Jr J T 1995 Photocatalysis on TiO$_2$ Surfaces: Principles, Mechanisms, and Selected Results, *Chem. Rev.* **95(3)** 735-58.

[2]   Akpan U G, Hameed B H, 2009 Parameters Affecting the Photocatalytic Degradation of Dyes Using TiO$_2$-Based Photocatalysts: A Review, *J. Hazard. Mater.* **170(2-3)** 520-9.

[3]   Daneshvar N, Salari D, Khataee A R 2004 Photocatalytic Degradation of Azo Dye Acid Red 14 in Water on ZnO as an Alternative Catalyst to TiO$_2$, *J. Photochem. Photobiol. A Chem.* **162(2-3)** 317-22.

[4]   Da Silva L F, Lopes O F, De Mendonça V R, Carvalho K T, Longo E, Ribeiro C, Mastelaro V R 2016 An Understanding of the Photocatalytic Properties and Pollutant Degradation Mechanism of SrTiO$_3$ Nanoparticles, *Photochem. Photobiol.* **92(3)** 371-8.

[5]   Han F, Li H, Fu L, Yang J, Liu Z 2016 Synthesis of S-Doped WO3 Nanowires with Enhanced Photocatalytic Performance towards Dye Degradation, *Chem. Phys. Lett.* **651** 183-7.

[6]   Hu W, Yuan X, Liu X, Guan Y, Wu X 2017 Hierarchical SnO2 Nanostructures as High Efficient Photocatalysts for the Degradation of Organic Dyes, *J. Sol-Gel Sci. Technol.* **84(2)** 316-22.

[7]   Atabaev T S, Ajmal M, Hong N H, Kim H K, Hwang Y H 2015 Ti-Doped Hematite Thin Films for Efficient Water Splitting, *Appl. Phys. A* **118(4)** 1539-42.

[8]   Qin D D, Li Y. L, Wang T, Li Y, Lu X Q, Gu J, Zhao, Y X, Song, Y M, Tao C L 2015 Sn-Doped Hematite Films as Photoanodes for Efficient Photoelectrochemical Water Oxidation, *J. Mater. Chem. A* **3(13)** 6751-5.

[9]   Barrero C A, Arpe J, Sileo E, Sánchez L C, Zysler R, Saragovi C 2004 Ni- and Zn-Doped Hematite Obtained by Combustion of Mixed Metal Oxinates, *Physica B: Conden. Matt.* **354(1-4)** 27-34.

[10]   Kleiman-Shwarsctein A, Hu Y S, Forman A J, Stucky G D, McFarland E W 2008 Electrodeposition of α-Fe$_2$O$_3$ Doped with Mo or Cr as Photoanodes for Photocatalytic Water Splitting, *J. Phys. Chem. C* **112(40)** 15900-7.